Made available by Hasselt University Library in https://documentserver.uhasselt.be

Diamond related materials for energy storage and conversion applications Peer-reviewed author version

Yu, Si-yu; Wang, Xi-yan & YANG, Nianjun (2025) Diamond related materials for energy storage and conversion applications. In: New Carbon Materials, 40 (4), p. 973-991.

DOI: 10.1016/S1872-5805(25)61021-3 Handle: http://hdl.handle.net/1942/47399

Diamond related materials for energy storage and conversion applications

Siyu Yu^{1,*}, Xiyan Wang¹, Nianjun Yang²

- 1. School of Chemistry and Chemical Engineering, Southwest University, Chongqing 400715, China
- 2. Department of Chemistry & IMO IMOMEC, Hasselt University, Diepenbeek 3590, Belgium

* Corresponding author

E-mail: yusiyu@swu.edu.cn

Abstract: Diamond combines many unique properties, including high stability, strong optical dispersion, excellent mechanical strength, and outstanding thermal conductivity. Its structure, surface groups, and electrical conductivity are also tunable, increasing its functional versatility. These make diamond and its related materials, such as its composites, highly promising for various applications in energy fields. This review summarizes recent advances and key achievements in energy storage and conversion, covering electrochemical energy storage (e.g., batteries and supercapacitors), electrocatalytic energy conversion (e.g., CO₂ and nitrogen reduction reactions), and solar energy conversion (e.g., photo-(electro)chemical CO₂ and nitrogen reduction reactions, and solar cells). Current challenges and prospects related to the synthesis of diamond materials and the technologies for their energy applications are outlined and discussed.

Key words: Diamond related materials; Electrochemical energy storage; Electrocatalytic energy conversion; Solar energy conversion; Future energy application directions

1 Introduction

Diamond, a metastable allotrope of carbon with a fully sp³-hybridized tetrahedral lattice, exhibits a unique combination of exceptional physical and chemical properties. As a wide-bandgap semiconductor (~5.5 eV), diamond features superior electrical insulation in its intrinsic state, yet can be precisely doped (e.g., with boron, nitrogen and phosphorus) to impart controlled p-type or n-type conductivity^[1, 2]. This tunability enables its application not only in high-power, high-frequency, and radiation-hard electronic devices, but also in electrochemical systems as robust electrodes. Additionally, diamond exhibits an ultra-wide electrochemical potential window, high thermal conductivity, extreme chemical inertness, and superior mechanical strength, rendering it a promising platform for energy applications, especially for those operating under harsh electrochemical and thermal environments.

During the past decades, various diamond materials (e.g., films and composites) have been artificially synthesized in a wide range of morphologies, including powders, micro- and nanocrystals, continuous polycrystalline or single-crystal films, and engineered nanostructures such as nanowires, nanopillars, and porous architectures^[3, 4]. This is thanks to the progress in chemical vapor deposition (CVD) techniques, including microwave plasma enhanced CVD, hot filament CVD, and direct-current arc plasma CVD ^[5, 6], which have enabled scalable and high-quality diamond growth with precise control over doping concentration, grain size, crystallographic orientation, and surface termination ^[7]. Large-area diamond nanostructures are typically fabricated using top-down etching or bottom-up growth methods, which may be implemented with or without the use of masks or templates. These various structural forms have been customized to meet specific functional requirements.

At the nanoscales of various diamond materials, they exhibit enhanced surface reactivity, allowing for functionalization with atoms or small groups such as hydrogen and oxygen functional groups (e.g., hydroxyl and carboxyl). These terminations influence key surface properties (e.g., polarity and wettability), and provide anchoring sites for further modification. Building on this functional versatility, diamond is often incorporated into composite systems with materials such as sp² carbon materials, transition metal particles, metal oxides, polymers, or organic molecules^[8-11]. These composites leverage the mechanical and electrochemical stability of diamond together with the complementary properties of the added phase(s), such as improved charge transport, redox activity, or light absorption, enabling synergistic performance in advanced energy storage and conversion applications.

This article thus provides a comprehensive overview of the emerging applications of

diamond and its composites in energy technologies. Specifically, three major areas are of interest: electrochemical energy storage, electrocatalytic energy conversion, and solar energy conversion. In addition, several potential future directions are outlined, covering photo-induced energy storage, energy applications at high-temperature, and the development of flexible energy devices.

2 Energy storage and conversion applications

2.1 Electrochemical energy storage

2.1.1 Batteries

Diamond materials have been applied as electrodes for the construction of advanced batteries, such as metal-air batteries^[12, 13], Li-ion and Li-metal batteries^[14-20], and sodium-ion and sodium-metal batteries^[21-27]. In these cases, they contributed to improved electrochemical stability, interface engineering, and structural integrity.

Metal-air batteries generate electricity through the oxidation of a metal anode, while oxygen from ambient air serves as the cathodic reactant. A flexible, binder-free cathode composed of Co₄N deposited on nitrogen-doped carbon nanowalls/diamond (NCNWs/D) was synthesized for the development of zinc-air batteries, demonstrating excellent bifunctional catalytic activity for both the oxygen reduction reaction (ORR) and oxygen evolution reaction (OER)[13]. In this architecture, NCNWs/D exhibited a three-dimensional network structure with a high surface area, enabling uniform dispersion of Co₄N nanoparticles, and thereby improving the density and accessibility of active sites. The strong covalent bonding between the diamond and carbon layers imparted high mechanical strength and flexibility, while the embedded diamond phase maintained structural integrity during synthesis steps such as electrochemical oxidation and high-temperature treatment. Notably, the diamond-carbon nanowall hybrid structure provided vertically aligned electron transfer pathways, lowering internal resistance and facilitating charge transfer during electrochemical reactions. Guided by density functional theory (DFT) calculations (Fig. 1a-d), the NCNWs/D substrate underwent electrochemical oxidation to introduce vacancy defects, which promoted the formation of Copyridinic nitrogen-carbon (N-C) bonds. These bonds enhanced charge transfer and reduced reaction energy barriers. The catalyst achieved a low OER overpotential of 340 mV at a current density of 10 mA cm⁻² and a high ORR half-wave potential of 0.83 V. When assembled with a zinc foil, the resulting zinc-air battery exhibited a high open-circuit voltage of 1.41 V and outstanding mechanical flexibility with stable performance under bending.

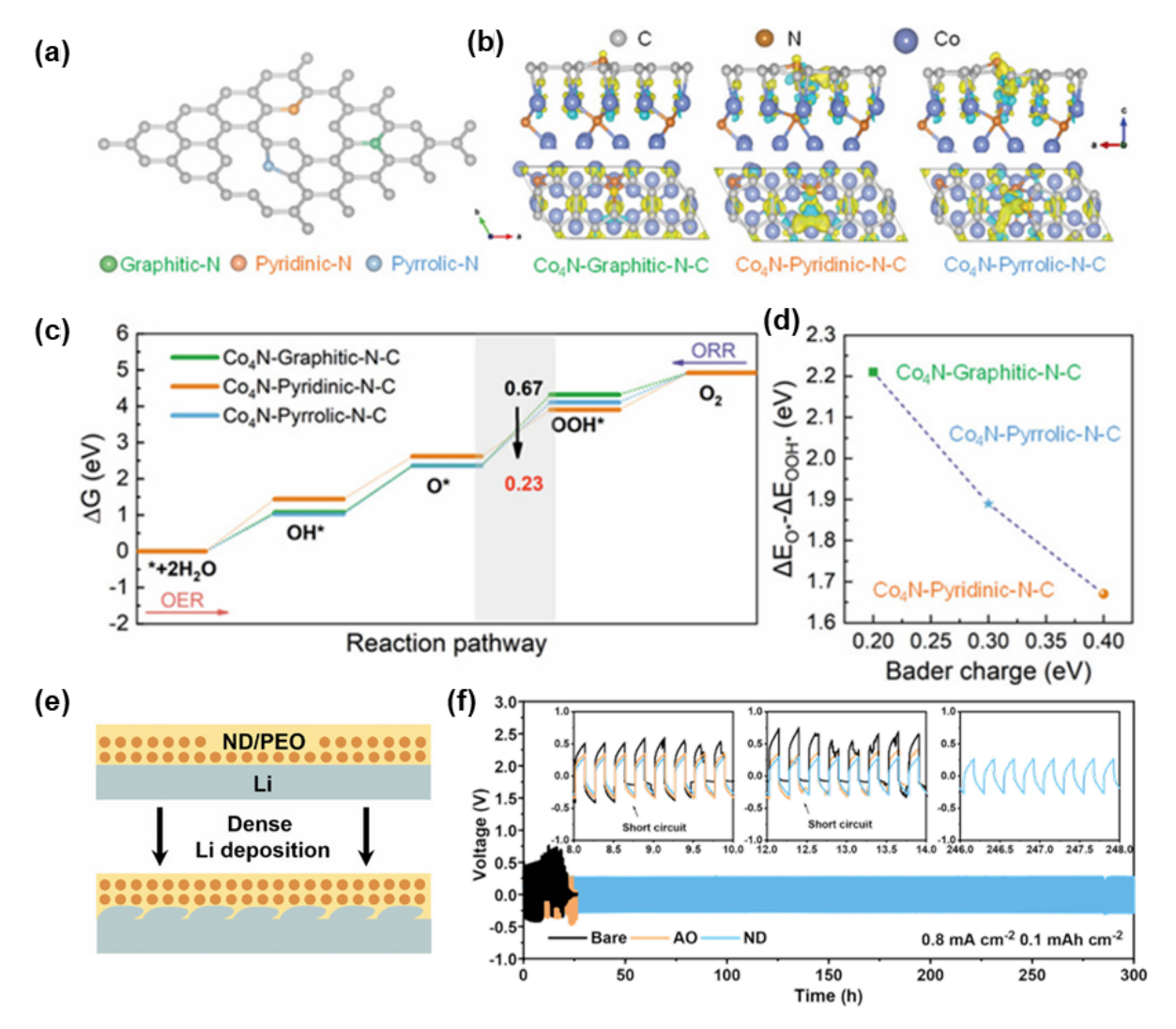


Fig. 1 Diamond materials for battery applications. (a-d) The DFT calculations of the interfaces with different N configurations: (a) different configurations of N dopants in graphene monolayers, (b) difference of charge densities on the interface of the Co₄N-Graphitic-N-C, Co₄N-Pyridinic-N-C, and Co₄N-Pyrrolic-N-C, (c) the calculated free energy diagrams for different ORR/OER pathways on the Co₄N-Graphitic-N-C, Co₄N-Pyridinic-N-C, and Co₄N-Pyrrolic-N-C, and (d) the relationship between the Bader charge and the free energy of rate-limiting step O*-OOH* on the Co₄N-Graphitic-N-C, Co₄N-Pyridinic-N-C, and Co₄N-Pyrrolic-N-C. Reproduced with permission^[13]. Copyright 2023 Wiley-VCH GmbH. (e-f) (e) Illustration of the Li morphology after long-term galvanostatic cycling of Li symmetric cell using the ND modified poly(ethylene oxide) (PEO) solid-state electrolyte, (f) long-term galvanostatic cycling profiles of Li symmetric batteries at 0.8 mA cm⁻² and 0.1 mAh cm⁻² using bare PEO, Al₂O₃ (AO) modified PEO, and ND modified PEO solid-state electrolytes. Reproduced with permission^[20]. Copyright 2022 Wiley-VCH GmbH.

Li-ion and Li-metal batteries are widely used and extensively studied due to their high energy density. In these systems, diamond materials provide unique benefits by stabilizing the electrode-electrolyte interface, suppressing side reactions, promoting uniform lithium deposition and inhibiting dendrite formation, thus contributing to improved cycling performance and safety. For example, incorporating 3.6 nm single-crystal diamond nanoparticles onto the silicon surface to form a double-layer Si/diamond/Si/diamond (Si/D/Si/D) structure as the anode in lithium-ion batteries demonstrated significant performance enhancements^[14]. The diamond surface and interfacial layers played crucial roles in homogenizing lithium-ion current density, thereby mitigating the formation of local "hot spots" that could cause excessive internal stress and eventual cracking of silicon thin films. The diamond nanoparticles also enhanced the hydrophilicity of the silicon surface, promoting uniform wetting by electrolytes and enabling the formation of a stable and homogeneous solid electrolyte interphase (SEI). This architecture supported uniform lithiation across the thinfilm electrode and effectively dispersed the charging-discharging current, preventing localized reactions that would otherwise lead to electrode polarization, stress concentration, and mechanical failure. Consequently, the diamond-modified anode exhibited reduced internal stress, improved SEI robustness, and greater physical integrity. Compared to conventional thin-film silicon anodes, the Si/D/Si/D structure delivered significantly enhanced electrochemical durability and superior reversible capacity retention under high-rate and longterm cycling conditions. The introduction of nanodiamonds (NDs) into the electrolytes of lithium battery systems has been demonstrated to effectively suppress dendritic lithium growth through multiple mechanisms. When added to conventional liquid electrolytes, NDs served as heterogeneous nucleation seeds, as lithium ions preferentially adsorbed onto their surfaces due to their higher binding energy compared to typical electrode materials (e.g., Cu). Their exceptionally low lithium diffusion energy barrier and small size promoted the formation of fine-grained, uniform lithium deposits. Moreover, this co-deposition process was reversible, as NDs could detach and re-disperse into the electrolyte during lithium stripping, maintaining a stable ND concentration and ensuring long-term cycling durability of the system^[19]. When incorporated into solid polymer electrolytes (SPEs), NDs with high Young's modulus and inherent rigidity mechanically deformed uneven lithium deposits, thereby mitigating the "tip effect", which concentrated Li+ flux at protrusions and accelerated dendrite growth. Additionally, NDs redistributed the electric field at the anode interface and facilitated the formation of dense, closely packed lithium deposits (Fig. 1e)[20]. In SPE-based lithium symmetric cells, this strategy extended the cycling lifespan by 30-fold at 0.8 mA cm⁻² (Fig.

1f). Furthermore, in high-voltage SPE-based Li/LiCoO₂ cells, it enabled excellent cycling performance, with 92.2% capacity retention after 50 cycles, while also effectively mitigating electrolyte degradation at the cathode.

Sodium-ion and sodium-metal batteries have attracted significant attention due to the abundance and low cost of sodium resources. NDs have been incorporated into electrodes^[21-23], electrolytes^[24, 25], and separators^[26-28] to enhance their performance through multiple synergistic effects. These include: (i) providing abundant electroactive sites for Na⁺ adsorption, thus increasing reversible capacity; (ii) promoting uniform Na⁺ deposition and facilitating the formation of a thin and stable SEI; (iii) reducing the activation energy of charge transfer at the electrode-electrolyte interface to improve reaction kinetics; (iv) suppressing dendritic growth to minimize the risk of short circuits; and (v) maintaining stable and efficient Na+ transport channels. For example, after NDs were integrated into a hard carbon anode derived from cattail grass, the modified anode delivered a high reversible capacity of 365.1 mAh g⁻¹ at 0.1 A g⁻¹ after 90 cycles at room temperature. Under low-temperature conditions (-40 °C), it retained a capacity of 245.1 mAh g⁻¹ at 0.1 A g⁻¹ after 90 cycles and maintained 108.2 mAh g⁻¹ at 1.0 A g⁻¹ after 500 cycles, corresponding to a capacity retention of 90%^[21]. The introduction of NDs into diglyme-based electrolytes also led to enhanced low-temperature performance of sodium-ion batteries. At -40 °C, the modified batteries exhibited an initial reversible capacity of 324 mAh g⁻¹, only slightly lower than that (357 mAh g⁻¹) recorded at room temperature, with a capacity retention of approximately 82% after 100 cycles at 0.1 A g⁻¹. Moreover, they maintained a capacity of 40 mAh g⁻¹ at 1 A g⁻¹ after 2000 cycles at -40 °C, nearly five times higher than that obtained with the pristine diglyme electrolyte under the same conditions^[24]. In another study, NDs were coated onto the surface of a glass fiber separator for sodium-ion batteries^[26]. The ND-modified separator showed enhanced Na⁺ transport and reduced interfacial resistance compared to the original separator. As a result, sodium-ion batteries with the ND-modified separator delivered a high reversible capacity of 483 mA h g⁻¹ at 50 mA g⁻¹ after 100 cycles, outperforming those with the traditional glass fiber separator (310 mA h g⁻¹).

2.1.2 Supercapacitors

Supercapacitors are another type of electrochemical energy storage devices. Compared to rechargeable batteries, SCs exhibit higher power density, faster charging-discharging rate, longer lifespan, yet lower energy density. Based on their charge storage mechanisms, SCs can be categorized into electrical double layer capacitors (EDLCs), pseudocapacitors (PCs), and redox-electrolyte enhanced SCs (R-SCs). EDLCs store charges through electrostatic charge

adsorption/desorption at the electrode surface, whereas PCs and R-SCs rely on Faradaic reactions of redox-active species immobilized on the electrode or dissolved in the electrolyte, respectively.

The capacitance of flat diamond film-based EDLCs is typically on the order of µF cm^{-2[29,} ^{30]}. Various strategies have been explored to enhance the performance of diamond based SCs, including the synthesis of novel diamond nanostructures and composites, as well as the development of advanced SC architectures such as R-SCs, asymmetric SCs (ASCs), and metal-ion capacitors. As SC electrodes, diamond nanostructures should ideally possess high specific surface area, tunable surface chemistry, and abundant adsorption sites. Different porous diamond electrodes have been synthesized, leading to an increase in EDLC capacitance to the order of mF cm⁻². These electrodes include porous boron-doped diamond (BDD)[31-34], BDD/SiO₂ fibers[35], BDD network[36, 37], BDD nanofeather[38], etc. For instance, multilayered porous BDD films were fabricated through repeated self-assembly seeding and short-time growth using microwave plasma enhanced CVD, achieving a high BET surface area (~350 m² g⁻¹) and thus an EDLC capacitance of up to 17.18 mF cm^{-2[31]}. A template-/maskfree method was also developed to produce 3D porous BDD networks by selective etching of β-SiC from diamond/β-SiC composite films. The resulting porous structure and enlarged active electrode area facilitated electrolyte penetration and shortened ion transport paths, yielding an EDLC capacitance of 3.53 mF cm^{-2[37]}. Additionally, anodic etching of BDD films in a mixture of acetic and sulfuric acid generated diamond nanofeathers with high-aspect-ratio porous architectures, delivering an EDLC capacitance of 3.1 mF cm^{-2[38]}.

Diamond-based composites have also been developed by integrating diamond with other functional materials, particularly carbon-based and pseudocapacitive materials. These composites combine the favorable properties of the constituent materials, for example, the high surface area of carbon materials and the high theoretical capacitance of pseudocapacitive materials. Diamond has been combined with various carbon materials such as carbon (nano)fiber or carbon cloth (CC)^[39, 40], graphite or graphene^[41,44], and carbon nanotubes^[45]. These hybrids not only enhance the electrochemical performance of diamond electrodes but also improve mechanical flexibility and structural integrity. For example, a vertical graphene/diamond composite film featuring regular and ordered 0.7-nm layered channels created a nanoconfined environment conducive to the formation of a layer-confined electrical double layer (EDL), leading to significantly enhanced capacitance^[42]. This system also served as an ideal model for studying confined EDL behavior both experimentally and theoretically. When BDD was coated onto CC, the resulting composite exhibited the flexibility of CC and

the stability of BDD^[39]. A quasi-solid-state EDLC fabricated using this diamond cloth demonstrated excellent mechanical resilience, retaining 97.14% of its capacitance after 500 bending cycles (0-180°).

Incorporating pseudocapacitive materials into diamond-based electrodes introduces Faradaic redox reactions during charging-discharging processes, which significantly enhances capacitance. However, this enhancement often comes at the cost of a narrower operating voltage window and potentially reduced device lifespan due to the degradation of pseudocapacitive materials or poor interfacial bonding with diamond electrodes. A wide variety of pseudocapacitive composites have been explored including MnO₂/BDD^[29, 46]. ZnO/BDD^[47], CoNiO₂/Co₃O₄/BDD^[48], Co-MOF derived Co₃O₄@BDD^[49], Bi-MOF derived Bi- Bi_2O_3 (@BDD^[49], Ni/NiCoP (@BDD^[50], TiC/BDD^[51], BDD/TiO₂ nanotube/Ti^[52], BDD/porous Ti^[53], BDD foam/Ta^[54], BDD/Ta fiber^[55], boron and nitrogen co-doped diamond/Ta/Ti/Si^[56], polyaniline/BDD/carbon fiber[57], etc. A particularly notable example involves the synthesis of a MnO₂/BDD composite via high-dose Mn ion implantation (10¹⁵-10¹⁷ ions cm⁻²) during BDD film growth, followed by post-annealing treatment^[46]. This process induced the formation of graphitized carbon and MnO₂ phases, both of which contributed significantly to charge storage. The resulting electrode demonstrated a markedly enhanced capacitance compared to pristine BDD electrodes, along with excellent cycle life, maintaining nearly 100% capacitance retention after 10 000 cycles in aqueous solution and approximately 80% after 88 000 cycles in a polymer gel electrolyte.

R-SCs further improve performance by incorporating soluble redox-active species into the electrolytes, where their Faradaic reactions contribute additional capacitance. Compared with PCs, R-SCs offer the advantages of simpler fabrication and greater flexibility in tuning the type and concentration of redox species. Redox additives such as $[Fe(CN)_6]^{3-/4}$, (ferrocenylmethyl)trimethylammonium hexafluorophosphate and ferrocene have been employed in diamond-based R-SCs^[30, 32, 37, 39-41, 43, 50, 58-60]. Notably, the introduction of $[Fe(CN)_6]^{3-/4}$ led to a three-order-of-magnitude increase in capacitance on nitrogen-incorporated BDD films^[60].

Another approach to enhance performance is the construction of asymmetric and hybrid SCs. By combining different electrode/electrolyte systems with varied potential windows, the overall working voltage of a SC device can be expanded. For instance, an aqueous ASC composed of Co-MOF derived Co₃O₄@BDD/KOH+[Fe(CN)₆]^{3-/4-} as the positive compartment and Bi-MOF derived Bi-Bi₂O₃@BDD/KOH as the negative compartment achieved an operating voltage of 1.7 V^[49]. Hybrid metal-ion capacitors, which pair battery-type and

capacitor-type electrodes, combine further the high energy density of batteries with the high power density of SCs. A Zn-ion capacitor assembled using diamond fibers (fibrous core/shell structured BDD/carbon fibers) as the positive electrode and zinc nanosheet coated diamond fibers as the negative electrode delivered a maximal energy density of 70.7 Wh kg⁻¹, a maximal power density of 4395.3 W kg⁻¹, and retained 89.9% of its capacitance after 10 000 cycles^[61]. A Na-ion capacitor based on boron-doped graphene/BDD/Ta achieved a high voltage of 3.2 V, a high energy density of 79.5 Wh kg⁻¹ at a power density of 221 W kg⁻¹, and a high power density of 18.1 kW kg⁻¹ at an energy density of 30.7 Wh kg⁻¹, along with excellent cycling stability^[62].

Through these approaches, diamond-based SCs can achieve energy and power densities comparable to or even surpassing those of other energy storage devices (Fig. 2).

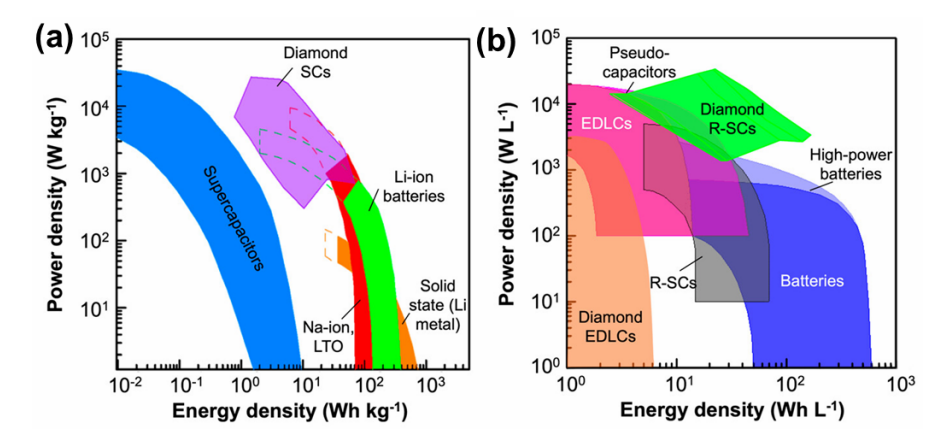


Fig. 2 Diamond materials for SC applications. Comparison of (a) gravimetric Ragone plots of diamond SCs and (b) their volumetric ones with those of other energy storage devices. Reproduced with permission^[63]. Copyright 2022 The Authors.

In short, the application of diamond materials in electrochemical energy storage systems illustrates their adaptability across fundamentally different charge storage mechanisms. Diamond materials exhibit multifunctionality, serving not only as robust electrode frameworks, but also as active participants in charge transport and interface regulation. Their chemical inertness, tunable conductivity, and structural versatility make them effective in mitigating degradation, enhancing electron/ion mobility, and maintaining consistent long-term performance. These advantages suggest that diamond could be further applied to emerging energy storage technologies, such as potassium-ion, aluminum-ion, and magnesium-ion batteries and capacitors. Compared to lithium, these alternative charge carriers are more abundant, less expensive, and in some cases safer, making them attractive for large-scale and sustainable energy storage applications. The interface control and structural benefits offered

by diamond materials may help address the challenges of compatibility and performance in these systems. Furthermore, the combination of diamond's physicochemical properties and electrochemical functionality underpins its potential for broader energy-related applications, including electrocatalysis.

2.2 Electrocatalytic energy conversion

Diamond and diamond-based materials have attracted growing interest in the field of electrocatalytic energy conversion, demonstrating promising performance in key reactions such as carbon dioxide reduction reaction (CO₂RR) and nitrogen reduction reaction (NRR), which enable efficient electrochemical conversion of CO₂ and N₂ into value-added products. This is primarily attributed to their wide electrochemical potential window, which effectively suppresses the competing hydrogen evolution reaction (HER). As a result, they offer enhanced Faradaic efficiency (FE) and product selectivity, while reducing energy consumption through more efficient electron utilization. Their outstanding stability under harsh electrochemical conditions further reinforces their potential for the development of efficient and durable energy conversion systems.

2.2.1 CO₂ reduction reaction

The performance of CO₂RR on diamond-based electrodes, in terms of Faradaic efficiency, product distribution, and selectivity, is strongly influenced by the intrinsic properties of the electrodes. These properties encompass the type and concentration of dopants, non-diamond carbon content, surface chemistry, morphology and incorporation of additional electrocatalytic components. Moreover, external factors such as the composition, pH, and concentration of the electrolyte, along with operational parameters like applied potential, current density, and mass transport conditions, also play critical roles in determining the reaction outcomes. A range of value-added products has been synthesized (Eq. 1), such as CO and hydrocarbons including HCOOH, HCHO, CH₃OH, CH₃CH₂OH, and CH₃COOH.

$$xCO_2 + y(H^+ + e^-) \rightarrow C_x H_{v-2n} O_{2x-n} + nH_2 O$$
 (1)

The BDD electrode predominantly yields HCOOH and CO in CO₂RR, with occasional reports of HCHO and CH₃OH formation. The catalytic activity of BDD is found to be dependent on the morphology/structure^[64-67] and surface state^[68-72]. For example, BDD films with varied surface morphologies, including flat, porous, and rough-surfaced BDD, were employed for electrochemical CO₂RR. The rough-surfaced BDD significantly outperformed the flat BDD, achieving a 1.7-fold increase in CO yield, attributed to its larger electroactive

area. In contrast, the porous BDD, despite possessing the largest real surface area, exhibited the lowest activity, likely due to CO₂ diffusion limitations within the pores^[64]. By replacing the dopant atoms in diamond, the electrochemical CO₂RR performance can be effectively tuned^[73]. Periodic DFT calculations were performed to evaluate the electrocatalytic activity of single and dual dopants (B, N, and P) on diamond surfaces for CO₂RR. The results revealed that double-doped configurations significantly lowered the reaction energy barriers compared to single dopants, with the B-N co-doping showing the most pronounced effect^[74]. It was also found that nitrogen co-doping in BDD electrodes significantly improved CO₂RR performance at relatively low negative potentials (-2.0 V vs. Ag/AgCl) by facilitating the adsorption of hydrogen atoms on the electrode surface. This promoted the formation of key reaction intermediates (e.g., *COOH or *OCHO) through proton-coupled electron transfer, enabling CO₂ activation without requiring CO₂ generation^[75].

An effective approach to improve the electrocatalytic performance of diamond electrodes is to couple them with other electrocatalysts that exhibit intrinsically high activity. In these hybrid systems, diamond acts both as an active electrocatalyst and as a support that suppresses side reactions like hydrogen evolution. The added catalysts contribute to higher current densities, improved reaction rates and product selectivity. This synergy not only enhances overall efficiency but also expands the range of accessible products. Reported modifiers include metals (e.g., Cu^[76]), metal alloys (e.g., Cu-Au^[77]), metal-derived compounds (e.g., MXene^[78, 79] and SnO-SnO₂/Ti₃C₂T_x^[80]), and organic molecules (e.g., cobalt phthalocyanine^[81], cobalt-coordinated tetracyanoquinodimethane^[82], and amine^[83]). For example, amine-functionalized BDD (NH2-BDD) electrodes exhibited up to an 8-fold enhancement in CO selectivity during electrochemical CO₂RR compared to pristine BDD electrodes (Fig. 3a)[83]. Moreover, the NH₂-BDD electrodes possessed a positively shifted onset potential (E_{red}) by approximately 400 mV, indicating facilitated CO₂ activation due to interaction with surface amine groups. *In-situ* attenuated total reflectance-infrared (ATR-IR) measurements confirmed the formation of C-N bonds between amine groups and CO₂, as shown by the decreased intensity of the carbonyl stretching peak (~1640 cm⁻¹) at more negative potentials (Fig. 3b-c). Mechanistically, CO production was favored between -1.20 and -1.70 V (vs. Ag/AgCl), where CO₂ captured via C-N bond was reduced, while at more negative potentials, free CO₂ reduction dominated, leading to HCOOH formation (Fig. 3d).

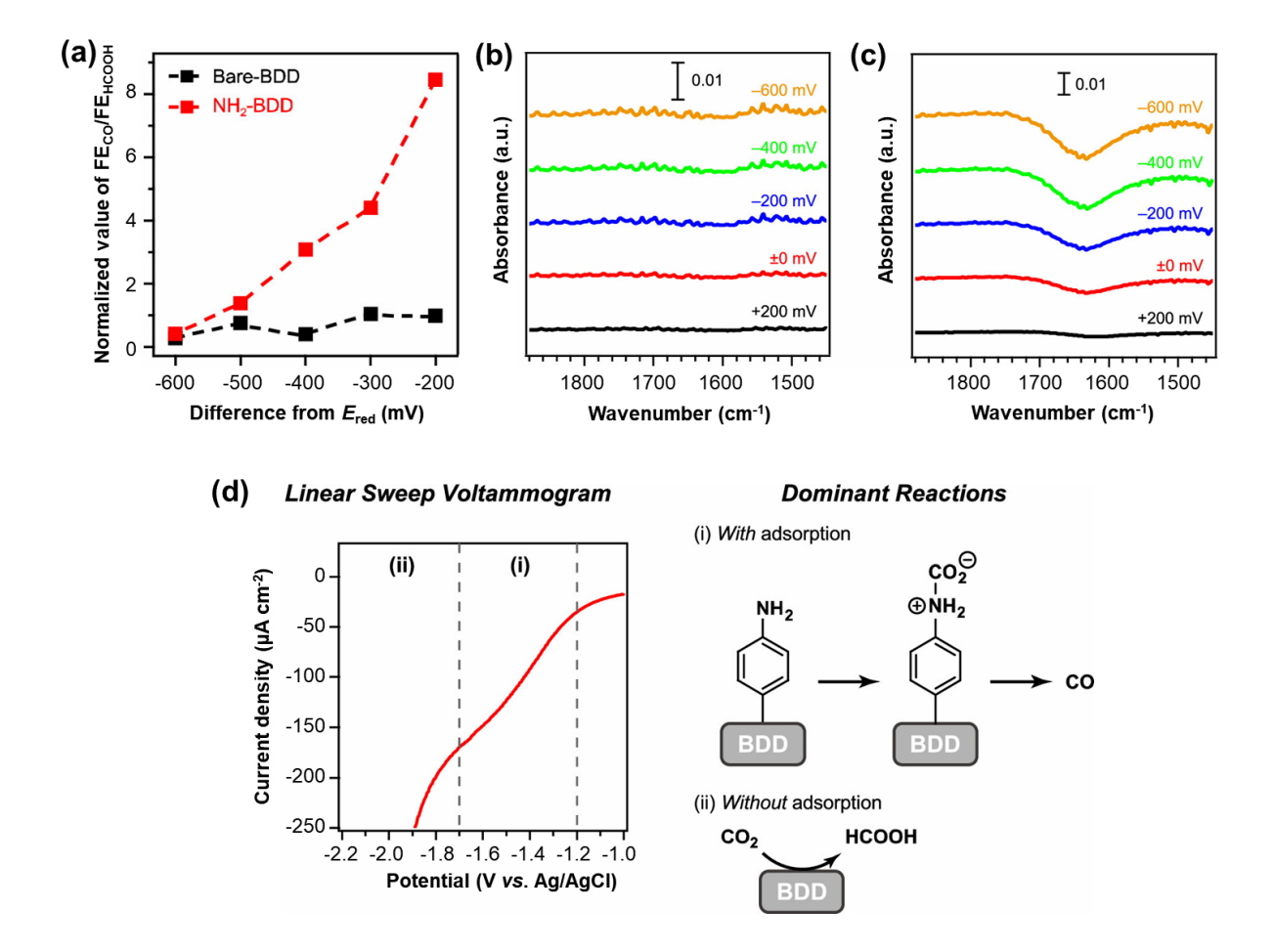


Fig. 3 Diamond materials for electrocatalytic applications. (a) Relationships between the selectivity of CO production and the difference from the E_{red} : (black) bare- and (red) NH₂-BDD. Values of FE_{CO}/FE_{HCOOH} were normalized to the value of bare-BDD obtained under an applied potential of 200 mV more negative than the E_{red} . The dashed lines are a guide for the eyes. (b-c) Potential-dependent ATR-IR spectra during electroreduction of CO₂ in KCl aqueous solution (0.5 M) on (b) bare-BDD and (c) NH₂-BDD. Applied potentials were swept from +200 to -600 mV referring to the reduction potential. (d) Postulated reaction pathways of CO₂ electroreduction on NH₂-BDD: (i) "with adsorption" pathway occurred at potentials between -1.20 and -1.70 V (vs. Ag/AgCl) and (ii) "without adsorption" pathway occurred at potentials more negative than -1.70 V (vs. Ag/AgCl). Reproduced with permission^[83]. Copyright 2022 American Chemical Society.

Some external factors, such as changes in electrolyte type and applied potential lead to variations in the FEs and main products obtained from electrochemical $CO_2RR^{[71, 75, 83]}$. In a single-compartment CO_2RR system employing a BDD cathode and a fluorinated polymer-topcoated IrO_2 anode, replacing the KCl electrolyte with K_2SO_4 increased the total FEs from 34.4% to $66.1\%^{[71]}$. Moreover, optimizing the applied electrode potential to -2.25 V (vs.

Ag/AgCl) further enhanced the FE for formic acid production. Mass transfer processes, including ion transport and convection, constitute the rate-determining step of CO₂RR, and thus have a significant impact on product selectivity and electrode potential^[84-86]. For example, the ion transport in the electrolyte, particularly the behavior of potassium (K⁺) and hydrogen ions (H⁺, pH), was closely monitored during long-term CO₂RR using a BDD electrode^[87]. A strong correlation was found between ion concentration dynamics and the stability of formic acid production. Based on these insights, a semi-permanent continuous production system was established by introducing a large initial amount of K⁺ and periodically replacing the electrolyte once the formic acid concentration reached 3.0 wt%. As a result, stable formic acid production was sustained for 1264 hours (approximately 53 days) with a Faradaic efficiency exceeding 70%.

2.2.2 N₂ reduction reaction

Compared to electrochemical CO₂RR, reports on diamond-based electrodes for electrochemical NRR under ambient conditions remain scarce, possibly due to the higher activation barrier and greater inertness of N₂ molecules compared to CO₂. The NRR process typically involves multiple proton-coupled electron transfer steps to convert N₂ into nitrogen-containing compounds such as NH₃.

The undoped ND electrode exhibited negligible NRR activity, whereas boron doping significantly activated the NRR. As the boron doping level increased, the NH₃ yield and FE initially improved due to the increased availability of active sites, but declined beyond an optimal point. This decline was attributed to enhanced HER at higher boron levels, caused by a lowered overpotential, which competed with NRR and reduced its selectivity^[88]. BDD nanocone films were further synthesized via reactive ion etching of BDD films and applied as efficient metal-free electrocatalysts for electrochemical NRR under ambient conditions. They achieved a high NH₃ yield rate of 19.1 µg h⁻¹ cm⁻² and a Faradaic efficiency of 21.2%, significantly surpassing pristine BDD films (4.1 µg h⁻¹ cm⁻² and 2.5%, respectively) under the same conditions, with stable operation over 8 days^[88]. The enhanced performance was attributed to the nanocone architecture, which intensified local electric fields and promoted surface charge accumulation, lowering the energy barrier for N₂ activation. DFT calculations revealed that diamond surfaces featuring low-coordinated sp³ carbon sites served as effective metal-free electrocatalysts for NRR[88]. Both the (111) and (110) surfaces were active for electrochemical NRR, with the (111) surface being more favorable due to its lower overpotential (0.57 V vs. 0.73 V) and stronger HER suppression, outperforming the benchmark Ru (0001) surface^[89].

The integration of diamond with other functional materials has further expanded its potential in NRR applications and research. A molybdenum oxide-modified BDD electrode also enabled efficient ambient NRR, exhibiting higher Faradaic efficiency (up to 9.15%), increased NH₃ yield, and lower overpotential compared to pure Mo electrodes, owing to the presence of high-valence Mo oxides^[90]. DFT calculations revealed that the BDD/Ni₄ interface exhibited excellent catalytic performance towards NRR, achieving a remarkably low overpotential of 0.27 V^[91]. The diamond substrate played a crucial role by providing strong adsorption energy and facilitating charge transfer to the Ni₄ cluster, which enhanced N₂ adsorption and activation. In particular, boron doping strengthened the binding between Ni₄ and diamond, stabilized the catalyst structure, and improved NRR activity by lowering energy barriers and preventing Ni aggregation. In contrast, H-terminal modifications on diamond hinder charge transport, reducing catalytic efficiency. Furthermore, a robust Au@BDD platform facilitated in-situ attenuated total reflection surface-enhanced infrared absorption spectroscopy studies of electrochemical NRR at -1.5 V (vs. Ag/AgCl), directly detecting both NH₃ and hydrazine under aqueous conditions^[92]. The chemically inert BDD layer withstood harsh electrolysis conditions that caused failure of conventional infrared-transparent internal reflection elements, enabling detailed spectroscopic insights into the associative NRR mechanism on the electrodes. Spectral analysis confirmed the formation and orientation of adsorbed hydrazine intermediates and the accumulation of dissolved ammonia, highlighting Au@BDD as a stable and effective surface-enhanced infrared substrate for probing electrocatalysis under strongly reducing conditions.

External factors have also been shown to influence the catalytic performance of diamond-based materials in NRR^[88, 90]. For instance, in the case of a BDD electrode, both the NH₃ yield rate and FE increased as the applied potential became more negative. However, further increasing the potential resulted in a notable decline in both metrics due to the enhanced competition from HER^[88].

Overall, recent advances in diamond-based electrocatalysts have demonstrated their great potential for CO₂RR and NRR. By tailoring crystal structure, heteroatom doping, surface functionalities, and integrating co-catalysts, researchers have developed a wide range of diamond-derived materials with tunable catalytic properties. External factors such as electrolyte composition and operating conditions have also been shown to influence catalytic performance. To further enhance conversion efficiency, product selectivity, and operational lifespan, while also reducing overpotentials and suppressing competing reactions like HER,

ongoing efforts are focused on the design of new catalyst structures, advanced electrode configurations, improved reactor systems, and optimized process control. These advancements are essential for enabling practical and scalable applications of diamond-based electrocatalytic systems.

2.3 Solar energy conversion

This chapter broadens the focus to solar energy conversion, which encompasses both photo-(electro)chemical catalytic processes and photovoltaic solar cells. Photo-(electro)chemical systems illustrate how light energy can be harnessed to drive catalytic reactions, effectively complementing traditional electrocatalysis. Meanwhile, solar cells represent a distinct but related strategy for harvesting solar energy, further expanding the scope of diamond-related energy technologies.

2.3.1 Photo-(electro)chemical CO₂RR and NRR

Diamond has emerged as a light-activated platform capable of emitting high-energy electrons to drive challenging multielectron reactions such as CO₂RR and NRR. Unlike electrocatalysis, which relies on an applied bias to inject electrons into a catalyst, photocatalysis with diamond utilizes photon absorption to generate electron-hole pairs that directly participate in surface redox reactions without external voltage. Photoelectrocatalysis offers a hybrid route where light enhances carrier generation while an external electrical connection further promotes charge separation and transport, improving both reaction rates and selectivity.

Hydrogen termination of diamond surfaces imparts negative electron affinity, enabling efficient electron emission under above-bandgap light illumination. This property is critical for generating solvated electrons in water, which can drive challenging reduction reactions such as CO₂RR and NRR. In contrast, oxygen-terminated diamond lacks negative electron affinity and exhibits negligible electron emission under similar conditions^[93]. Experimental data confirmed that only H-terminated BDD showed detectable NH₃ production, highlighting the essential role of surface termination in facilitating electron transfer into aqueous media and enabling photocatalytic reactivity.

Pristine diamond possesses an ultrawide bandgap of 5.5 eV, which typically limits its light absorption to the deep UV region (λ < 225 nm). To extend its photoresponse into the visible range, various strategies have been developed, including defect engineering and integration with metallic materials^[94, 95]. For instance, nitrogen doping in diamond introduced

nitrogen-vacancy centers, which created mid-gap states that absorbed visible light and promoted electron excitation from defect levels to the conduction band, thereby boosting photocatalytic activity for NRR^[96]. Embedding Ag nanoparticles into diamond films significantly enhanced light absorption through plasmonic resonances and internal photoemission, allowing electrons from Ag to be injected into the diamond's conduction band^[97]. These Ag-embedded diamond films demonstrated a nearly 5-fold increase in NH₃ production under sub-bandgap excitation. Additionally, hydrogen-terminated, n-doped diamond grown on molybdenum substrates leveraged a metal-assisted absorption mechanism, where visible light was absorbed through the underlying metal, enabling photoemission at photon energies as low as 1.5 eV^[98]. The negative electron affinity of the diamond surface facilitated the emission of photogenerated electrons into aqueous solution, driving nitrogen reduction under mild, visible-light conditions.

A dual-compartment H-cell setup is commonly used to separate the reduction and oxidation half-reactions into two physically distinct chambers, enhancing overall efficiency and control. A simple setup connected a diamond cathode with a non-diamond anode (e.g., Pt) via an external wire to complete the circuit^[99, 100]. This design alleviated the problem of inefficient water oxidation on diamond surface by replacing it with a kinetically favorable oxidation reaction at the anode (e.g., oxidation of iodide to triiodide or Na₂SO₃ to Na₂SO₄). Charge neutrality was maintained by matching the rates of reduction and oxidation reactions, allowing electron emission from the diamond to proceed at its optimal rate. An H-cell integrated with a three-electrode system was also employed to apply an external bias (Fig. 4a)[95]. Applying a negative bias to a diamond platelet composed of nitrogen doped detonationsynthesized nanodiamond (DND) surface layers on a BDD bulk enhanced electron flow from the bulk to the surface, promoting charge separation under visible light (Fig. 4b). The p-n junction formed between the boron and nitrogen doped layers facilitated the emission of excited electrons through the hydrogen-terminated surface into a CO₂-saturated aqueous solution. This favorable band alignment and built-in electric field suppressed recombination, lowered the effective energy barrier for electron emission, shifted the flat-band potential, and improved electron transfer directionality and efficiency, consequently enabling more efficient visible-light-driven CO₂ reduction to CO.

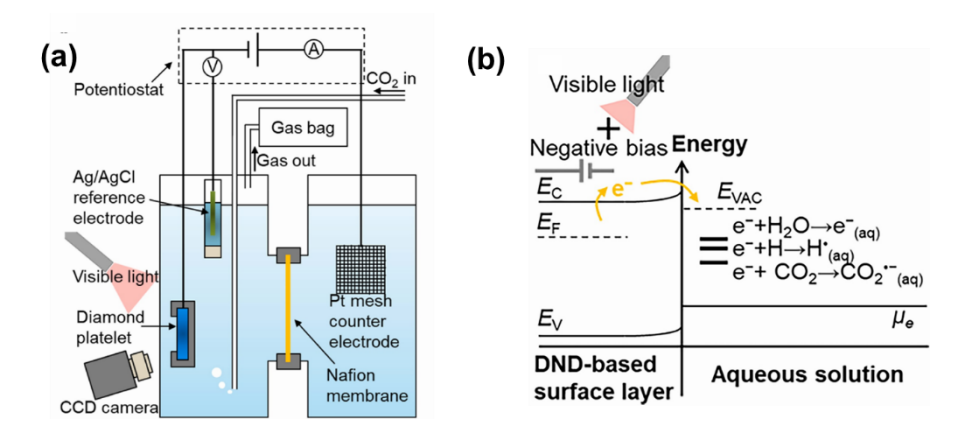


Fig. 4 Diamond materials for photo-electrochemical applications. Photo-electrochemical CO_2RR on a diamond platelet composed of nitrogen doped DND surface layers on a BDD bulk: (a) schematic of the H-type quartz cell with a three-electrode system, (b) energy diagram of the electron-excitation surface layer with the assumed chemical potential of CO_2 -saturated aqueous solution (μ_e) and relevant redox potentials on absolute energy scale converted from their electrochemical potentials versus standard hydrogen electrode under visible light irradiation with a negative bias applied. Reproduced with permission^[95]. Copyright 2023 Daicel Corporation, Kanazawa University.

2.3.2 Solar cells

Solar cells are devices that convert sunlight directly into electricity through the photovoltaic effect, where absorbed photons generate electron-hole pairs that are separated by an internal electric field to produce current. Diamond has emerged as a promising material for solar cells due to its exceptional properties, including a wide bandgap, high carrier mobility, excellent thermal conductivity, and outstanding radiation hardness. A novel ND/zinc nanocomposite counter electrode was fabricated using a simple drop-casting method for flexible dye sensitized solar cells, demonstrating performance comparable to or exceeding that of platinum, with a 6.23% efficiency enhancement at an optimal 8% zinc concentration^[101]. ND particles were also introduced to modify the CsPbIBr₂/carbon interface in planar all-inorganic perovskite solar cells, effectively enhancing film quality by filling surface pinholes and passivating grain boundaries[102]. As a result, the device performance improved significantly, with the power conversion efficiency increasing from 7.46% to 9.07%, accompanied by enhancements in open-circuit voltage, short-circuit current density, fill factor, and long-term reliability. Diamond can also serve as a chemically and mechanically stable protective layer for photoanodes. For example, a CsPbBr₃-based perovskite photoanode protected with BDD carrying Ni nanopyramids and NiFeOOH maintained 97% of its initial photocurrent after 210 h of continuous operation in aqueous electrolytes, demonstrating record long-term performance among perovskite-based photoanodes under such conditions^[103].

Advancements in surface and structural engineering, such as nanotexturing, chemical functionalization, and molecular modification, have further expanded the potential of diamond materials for solar energy applications. Black diamond, produced by femtosecond laser treatment of native transparent diamond, exhibits higher solar absorptance and broader spectral response than untreated diamond^[104]. This improvement arises from enhanced light trapping and the formation of laser-induced energy levels within the bandgap, enabling more efficient absorption of sub-bandgap photons. Using a double-step femtosecond laser process, double-nanotextured black diamond films with a "2D-like" pseudo-periodic nanostructure were fabricated^[105]. These films achieved a remarkable solar absorptance of 99.1% across the 200 – 2 000 nm wavelength range.

In addition to structural texturing, the tunable surface chemistry of NDs enables control over work function and interfacial interactions with surrounding materials or environments^[106]. High-pressure high-temperature NDs (HPHT NDs) with different surface terminations demonstrated distinct charge extraction properties in organic solar cells (**Fig. 5a-d**)^[107]. Asreceived (HPHT ND-ar) and oxidized (HPHT ND-O) NDs possessed oxygen-rich surfaces and high work functions (~5.3 eV), theoretically suitable for hole extraction. However, their insulating nature hindered effective charge transport, leading to poor device performance. In contrast, hydrogenated NDs (HPHT ND-O-H), with a lower work function (~4.5 eV), were suitable for electron extraction in inverted device architectures. Devices using HPHT ND-O-H as the electron transport layer achieved up to 85% of the performance of those with conventional ZnO layers.

Diamond also integrates well with a wide range of photoactive materials, including conjugated polymers (e.g. polypyrrole^[106, 108]) and dye-sensitized molecules (e.g., dithienopyrrole-benzothiadiazole^[109]), broadening their utility in diverse solar cell architectures. In one study, a series of oligothiophene-perylene diimide (nT-PDI) donor-acceptor chromophores with varying spacer lengths were synthesized and covalently grafted onto BDD surface (**Fig. 5e**) for use in organic photovoltaic systems^[110]. This molecular modification was designed to optimize energy level alignment and charge transfer efficiency at the diamond-organic interface. Results showed that increasing the oligothiophene spacer length enhanced charge separation due to greater spatial separation of photoexcited charges. However, the highest photovoltage was observed with an intermediate chain length (3T-PDI), representing the optimal balance between charge separation and charge transport.

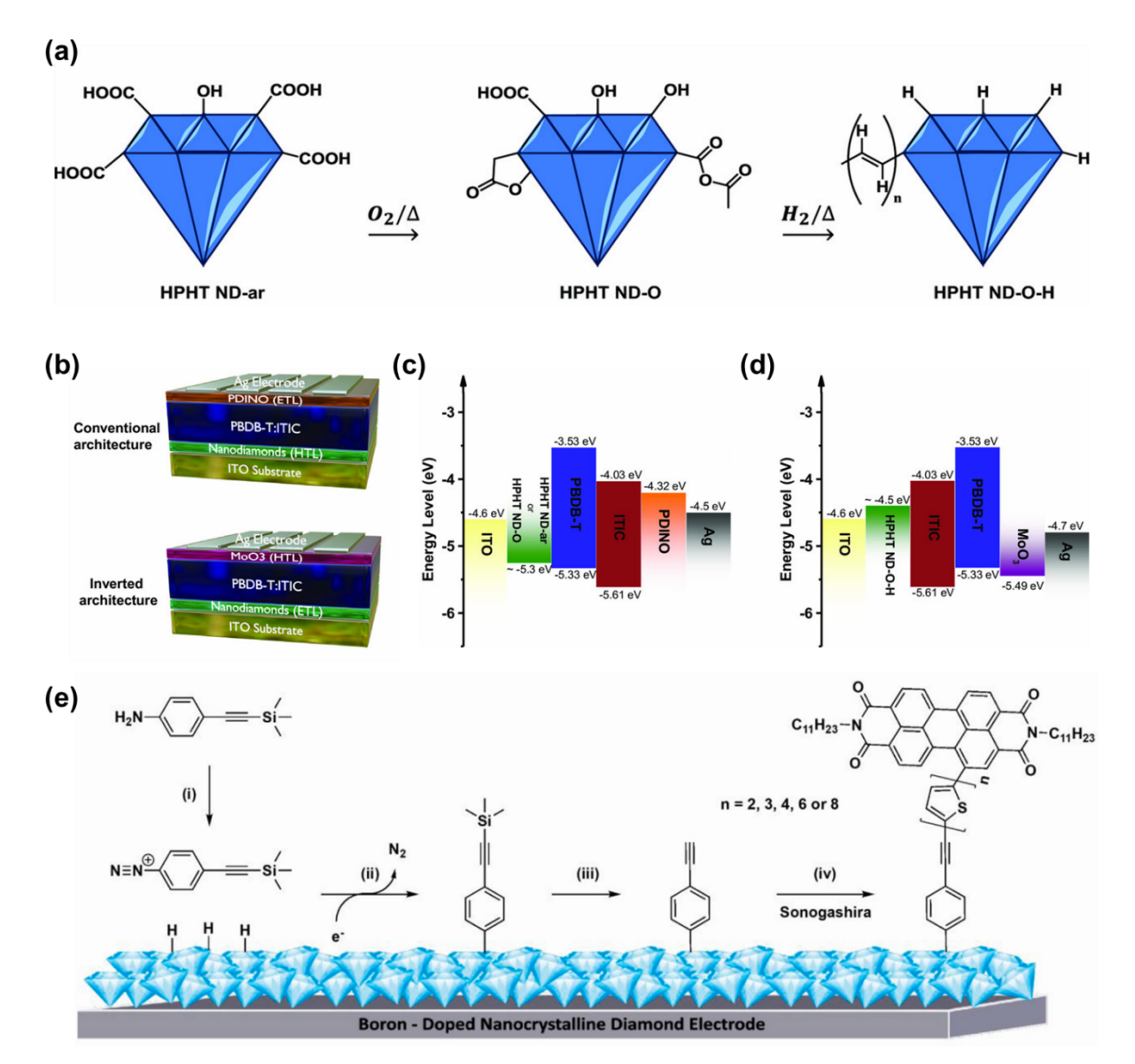


Fig. 5 Diamond materials for solar energy applications. (a-d) (a) surface chemistries of HPHT ND-ar, HPHT ND-O, and HPHT ND-O-H, (b) device architectures of the fabricated solar cells (top: conventional stack, bottom: inverted stack), energy level diagrams of the fabricated solar cells with (c) conventional architecture and (d) inverted architecture. Reproduced with permission[107]. Copyright 2023 The Authors. (e) functionalization strategy for the sensitization of BDD with nT-PDI chromophores (the chains are omitted here for clarity): diazotization (i) (trimethylsilyl)ethynylaniline, (ii) electrochemical reduction and subsequent grafting of the corresponding diazonium salt, (iii) removal of the trimethylsilyl groups with tetrabutylammonium fluoride, and (iv) dye sensitization of diamond via Sonogashira crosscoupling with iodinated nT-PDI. Reproduced with permission[110]. Copyright 2022 Elsevier B.V.

This chapter highlights the multifaceted roles of diamond materials in solar energy conversion, covering both photo-(electro)chemical catalysis and photovoltaic applications. In photo-(electro)chemical CO₂RR and NRR, diamond serves as a light-activated electron source, with its surface termination, doping, and hybrid structures playing critical roles in enhancing visible-light responsiveness and reaction selectivity. Reactor configurations like Hcells further improve performance by optimizing charge flow and reaction environments. In solar cells, diamond contributes as an active layer, interface modifier, or protective coating, improving device durability, charge transport, and light-harvesting efficiency. Surface and structural engineering strategies have been employed to boost solar absorption and tailor interfacial electronic properties. Research is expected to further explore diamond's potential in broadband light absorption, quantum efficiency enhancement, and photocatalytic stability under harsh conditions. The integration of diamond with emerging materials, such as perovskites, 2D semiconductors, or upconversion systems, may open new avenues for synergistic performance in solar-driven applications. These developments reflect a growing trend toward the multifunctional integration of diamond in solar energy systems, enabling both catalytic and photovoltaic functionalities within a unified platform.

3 Perspectives

Substantial progress has been achieved in the synthesis and applications of diamond materials, especially nanostructured and composite forms for different energy applications in the past decades. However, several critical challenges still hinder their broader utilization in energy technologies. The wide structural diversity of diamond, including nanoparticles, dense films, porous frameworks, and patterned nanostructures, offers significant potential for tuning material properties. Note that realizing this potential requires synthetic approaches that can precisely control crystal orientation, grain size, film uniformity, surface area, electrical conductivity, and interfacial characteristics in a scalable and reproducible manner. The surface chemistry of diamond plays a crucial role in influencing its bulk chemical and electrochemical properties. The effects of different surface terminations on electron transport, adsorption processes, and chemical durability must be systematically clarified. Progress in this area will rely on the combined use of *in-situ* characterization techniques and theoretical modeling to capture the dynamic structural and chemical evolution during both synthesis and device operation. Incorporating diamond into composite systems with other materials such as

carbon-based nanostructures, metal derived compounds, and conductive polymers has demonstrated enhanced performance through synergistic effects. Nonetheless, achieving uniform dispersion, stable interfaces, and chemical compatibility under practical conditions remains a major challenge. Further work is needed to tailor the chemical and structural integration at the nanoscale, including strategies for lattice matching, interface passivation, and stress management with the aid of machine learning or artificial intelligence in some situations.

Looking forward, the development of other diamond materials with targeted properties through controlled synthesis might represent an important opportunity. This goal depends on a comprehensive understanding of the detailed relationships between synthesis conditions, resulting structure, and performance in desired applications. The integration of *in-situ* monitoring techniques, multiscale simulations, and data-driven process optimization may enable the predictive design of diamond structures with specific functionalities. These advances will ultimately support the deployment of diamond materials in high-performance electrochemical energy storage, efficient catalytic conversion, and solar energy utilization.

Some potential future directions for diamond-based materials in energy applications include photo-induced energy storage systems, high-temperature energy systems, and flexible energy devices. Photo-induced energy storage devices, such as photo-supercapacitors and photo-rechargeable batteries, aim to integrate solar energy harvesting and energy storage within a single platform. These systems offer simplified architectures, reduced energy loss associated with multi-step processes, and the potential for real-time, on-demand energy capture and storage. However, they face several challenges, including inefficient light-tocharge conversion, poor charge separation, limited material stability under irradiation, and mismatches between energy conversion and storage components. Diamond related materials offer a compelling solution owing to their unique combination of properties applicable to both solar energy conversion units (e.g., photoelectrodes and solar cells) and energy storage elements (e.g., electrochemical electrodes). For example, hydrogen-terminated or doped diamond can exhibit surface conductivity and support photoinduced charge carrier generation, especially when combined with appropriate surface engineering or integrated with lightabsorbing semiconductors. In addition, diamond electrodes are chemically and electrochemically stable, and optically transparent, enabling operation under harsh conditions without degradation. In short, the intrinsic properties of diamond make it a versatile scaffold for designing hybrid devices that can overcome the common trade-offs between efficiency and long-term performance in photo-induced energy storage systems.

In energy applications at high temperatures, diamond provides a unique combination of exceptional thermal conductivity, outstanding thermal stability, and remarkable chemical inertness, suggesting that it could be a viable material platform for thermally resilient energy systems. However, further studies are needed to evaluate its practical integration and performance in such systems. To capitalize on these advantages, exploring nanostructured and doped diamond configurations warrants investigation, as they may offer enhanced control over thermal and electronic transport mechanisms under demanding conditions. Future research should also focus on optimizing the structural integration of diamond with thermally stable functional materials that can maintain their integrity at elevated temperatures while enabling efficient energy conversion or storage.

The development of flexible energy devices is another compelling and rapidly growing direction, particularly for applications in wearable electronics, portable sensors, and integrated self-powered systems. A key challenge in this area lies in preserving the excellent performance of diamond while introducing mechanical flexibility, which bulk or rigid diamond substrates inherently lack. This issue can be addressed by integrating nanostructured diamond films with flexible substrates like carbon cloth. To broaden the range of potential applications, it is important to explore alternative and multifunctional substrates (e.g., biodegradable polymers and transparent flexible films). Additional efforts are needed to improve film adhesion, enhance interfacial interaction between diamond and the substrate, and ensure long-term mechanical stability in flexible configurations. Moreover, the development of scalable fabrication strategies (e.g., direct low-temperature diamond growth on flexible substrates); will be essential for the realization of large-area and industrially relevant device production.

4 Conclusion

Diamond exhibits a wide electrochemical potential window and outstanding stability even under harsh conditions. Its performance can be modulated through various structural and compositional strategies. Taking nanostructuring as an example, it increases surface area and exposes more active sites, while doping alters electrical conductivity and introduces beneficial structural defects. Surface termination influences properties such as wettability, negative electron affinity, and surface chemistry. In addition, the presence of non-diamond sp² carbon phases can adjust electron transfer dynamics. The incorporation of diamond with other materials possessing different characteristics can impart new functionalities (e.g.,

pseudocapacitive behavior, mechanical flexibility, and an extended light absorption range), thereby significantly expanding its application potential. Diamond and its composites offer significant promise for efficient and durable energy conversion and storage systems. These include electrochemical energy storage devices such as batteries and supercapacitors, electrocatalytic systems for converting CO₂ and nitrogen into value-added products, and solar energy conversion technologies. A deeper understanding of the relationships among synthesis parameters, material structure, and functional performance is essential for achieving targeted design and optimization. Future research may focus on areas such as photo-induced energy storage, high-temperature energy systems, and flexible energy devices, which represent exciting directions for further development. It should also be noted that the volume of research specifically focused on diamond-based materials for energy applications remains relatively limited compared to the extensive studies on other carbon-based materials such as activated carbon and carbon nanotubes. This can largely be attributed to the complexity of diamond synthesis, which typically requires advanced instrumentation and stringent growth conditions, as well as the relatively high production cost that limits scalability and commercial application. However, with the continued development of CVD technology, the production of high-quality and lower-cost diamond materials has become more accessible and may facilitate broader utilization in the near future.

Acknowledgement

S. Yu acknowledges the financial support from Fundamental Research Funds for the Central Universities (Grant No. SWUKT22030), and Scientific and Technological Research Program of Chongqing Municipal Education Commission of China (No. KJQN202300205). N. Yang thanks the financial support from Deutsche Forschungsgemeinschaft (DFG, German Research Foundation, No. 457444676).

References

- [1] Guo T, Yang N, Yang B, et al. Electrochemistry of nitrogen and boron Bi-element incorporated diamond films[J]. Carbon, 2021, 178: 19-25.
- [2] Zhang X, Wang Y, Gai Z, et al. Synthesis of graphene interlayer diamond films for enhanced electrochemical performance[J]. Carbon, 2022, 196: 602-611.
- [3] Yang N, Yu S, Macpherson J.V, et al. Conductive diamond: synthesis, properties, and electrochemical applications[J]. Chemical Society Reviews, 2019, 48(1): 157-204.

- [4] Yu S, Yang N, Liu S, et al. Diamond supercapacitors: progress and perspectives[J]. Current Opinion in Solid State and Materials Science, 2021, 25(3): 100922.
- [5] Song Y M, Qiu S X, Feng S X, et al. A review of carbon nanotubes in modern electrochemical energy storage[J]. New Carbon Materials, 2024, 39(6): 1037-1074.
- [6] Feng X, Yuan X, Zhou J, et al. A review: CNT/diamond composites prepared via CVD and its potential applications[J]. Materials Science in Semiconductor Processing, 2025, 186: 109008.
- [7] Yang N, Krueger A, Hamers R J. Diamond chemistry: Advances and perspectives[J]. Angewandte Chemie International Edition, 2025, 64(25): 202418683.
- [8] Jian Z, Heide M, Yang N, et al. Diamond fibers for efficient electrocatalytic degradation of environmental pollutants[J]. Carbon, 2021, 175: 36-42.
- [9] Jian Z, Yang N, Vogel M, et al. Tunable photo electrochemistry of patterned TiO₂/BDD heterojunctions[J]. Small Methods, 2020, 4(9): 2000257.
- [10] Chen X, Dong X, Jiang X, et al. Diamond composite: A "1 + 1 > 2" strategy to design and explore advanced functional materials[J]. Accounts of Materials Research, 2024, 5(3): 295-306.
- [11] Zhai Z, Zhang C, Chen B, et al. Covalently bonded diaphite nanoplatelet with engineered electronic properties of diamond[J]. Advanced Functional Materials, 2024, 35(21): 2401949.
- [12] Huang H, Liu Q, Lu B, et al. LaMnO₃-diamond composites as efficient oxygen reduction reaction catalyst for Zn-air battery[J]. Diamond and Related Materials, 2019, 91: 199-206.
- [13] Zhang C, Huang N, Zhai Z, et al. Bifunctional oxygen electrocatalyst of Co₄N and nitrogen doped carbon nanowalls/diamond for high performance flexible zinc-air batteries[J]. Advanced Energy Materials, 2023, 13(41): 2301749.
- [14] Tzeng Y, Jhan C Y, Sung S H, et al. Effects of crystalline diamond nanoparticles on silicon thin films as an anode for a lithium-ion battery[J]. Batteries, 2024, 10(9): 321.
- [15] Lee E, Salgado R A, Lee B, et al. Design of lithium cobalt oxide electrodes with high thermal conductivity and electrochemical performance using carbon nanotubes and diamond particles[J]. Carbon, 2018, 129: 702-710.
- [16] Cheng Y W, Pandey R K, Li Y C, et al. Conducting nitrogen-incorporated ultrananocrystalline diamond coating for highly structural stable anode materials in lithium ion battery[J]. Nano Energy, 2020, 74: 104811.
- [17] Cheng Y W, Lin C K, Chu Y C, et al. Electrically conductive ultrananocrystalline diamond coated natural graphite copper anode for new long life lithium ion battery[J].

- Advanced Materials, 2014, 26(22): 3724-3729.
- [18] Liu Y, Tzeng Y K, Lin D, et al. An ultrastrong double-layer nanodiamond interface for stable lithium metal anodes[J]. Joule, 2018, 2(8): 1595-1609.
- [19] Cheng X B, Zhao M Q, Chen C, et al. Nanodiamonds suppress the growth of lithium dendrites[J]. Nature Communications, 2017, 8(1): 336.
- [20] Guo J, Zhang W, Shen Z, et al. Tuning ion/electron conducting properties at electrified interfaces for practical all solid state Li-metal batteries[J]. Advanced Functional Materials, 2022, 32(35): 2204742.
- [21] Zhao M, Zhang X, Li Z, et al. Enhancing the low-temperature performance of sodium-ion battery by introducing nanodiamonds in anode prepared from cattail grass[J]. Small, 2025, 21(15): 2410866.
- [22] Xu S, Feng J, Jiao M, et al. Preparation of nanodiamonds modified hard carbon with uniform spherical feature for improving sodium-ion storage performances[J]. Solid State Ionics, 2024, 410: 116546.
- [23] Zhai X, Feng J, Sun X, et al. Nanodiamonds in bio-carbon anodes realizing high performances of sodium-ion batteries[J]. Journal of Alloys and Compounds, 2023, 933: 167621.
- [24] Zhang X, Zhao M, Zhai X, et al. Nanodiamond-assisted high-performance sodium-ion batteries with weakly solvated ether electrolyte at -40 °C[J]. Small Methods, 2025, 9(3): 2400865.
- [25] Zhai X, Sun X, Zhang X, et al. Introducing nanodiamond-modified electrolyte to realize high capacity and rate performance of sodium ion batteries[J]. Journal of Power Sources, 2024, 622: 235358.
- [26] Zhai X, Sun X, Zhao M, et al. Boosting performances of sodium-ion battery by employment of nanodiamond modified separator[J]. Journal of Energy Storage, 2024, 101: 113745.
- [27] Li A, Wang H, Liu X, et al. Enhanced stability of sodium anodes by amino-functioned macroporous two-dimensional nanodiamond coated polypropylene separators[J]. Chemical Engineering Journal, 2024, 491: 151914.
- [28] Sun X, Gao X, Su C, et al. Nanodiamond assisted high performance lithium and sodium ions co storage[J]. Energy & Environmental Materials, 2024, 7(6): 12749.
- [29] Yu S, Yang N, Zhuang H, et al. Electrochemical supercapacitors from diamond[J]. Journal of Physical Chemistry C, 2015, 119(33): 18918-18926.
- [30] Yu S, Xu J, Kato H, et al. Phosphorus-doped nanocrystalline diamond for supercapacitor

- application[J]. ChemElectroChem, 2019, 6(4): 1088-1093.
- [31] Wang J, He Z, Tan X, et al. High-performance 2.6 V aqueous symmetric supercapacitor based on porous boron-doped diamond via regrowth of diamond nanoparticles[J]. Carbon, 2020, 160: 71-79.
- [32] Wang J, He Z, Tan X, et al. Hybrid supercapacitors from porous boron-doped diamond with water-soluble redox electrolyte[J]. Surface & Coatings Technology, 2020, 398: 126103.
- [33] Wang J, He Z, Tan X, et al. Achieving high capacitance from porous boron-doped diamond by tuning the surface termination[J]. Surface & Coatings Technology, 2021, 408: 126814
- [34] Suman S, Sharma D K, Szabo O, et al. Vertically aligned boron-doped diamond nanostructures as highly efficient electrodes for electrochemical supercapacitors[J]. Journal of Materials Chemistry A, 2024, 12(32): 21134-21147.
- [35] Vlčková Živcová Z, Mortet V, Taylor A, et al. Electrochemical characterization of porous boron-doped diamond prepared using SiO₂ fiber template[J]. Diamond and Related Materials, 2018, 87: 61-69.
- [36] Zhuang H, Yang N, Fu H, et al. Diamond network: template-free fabrication and properties[J]. ACS Applied Materials & Interfaces, 2015, 7(9): 5384-5390.
- [37] Yu S, Yang N, Zhuang H, et al. Battery-like supercapacitors from diamond networks and water-soluble redox electrolytes[J]. Journal of Materials Chemistry A, 2017, 5(4): 1778-1785.
- [38] Zeng H, Moldovan N, Catausan G. Diamond nanofeathers[J]. Diamond and Related Materials, 2019, 91: 165-172.
- [39] Li C, Dong X, Zhai Z, et al. High-performance flexible supercapacitors using diamond cloth[J]. Journal of Physical Chemistry C, 2025, 129(14): 6618-6627.
- [40] Yu S, Yang N, Vogel M, et al. Battery like supercapacitors from vertically aligned carbon nanofiber coated diamond: design and demonstrator[J]. Advanced Energy Materials, 2018, 8(12): 1702947.
- [41] Yu S, Sankaran K.J, Korneychuk S, et al. High-performance supercabatteries using graphite@diamond nano-needle capacitor electrodes and redox electrolytes[J]. Nanoscale, 2019, 11(38): 17939-17946.
- [42] Chen B, Zhai Z, Huang N, et al. Highly localized charges of confined electrical double-layers inside 0.7-nm layered channels[J]. Advanced Energy Materials, 2023, 13(36): 2300716.
- [43] Banerjee D, Sankaran K J, Deshmukh S, et al. Single-step synthesis of core-shell diamond-graphite hybrid nano-needles as efficient supercapacitor electrode[J]. Electrochimica Acta, 2021, 397: 139267.

- [44] Deshmukh S, Jakobczyk P, Ficek M, et al. Tuning the laser induced processing of 3D porous graphenic nanostructures by boron doped diamond particles for flexible microsupercapacitors[J]. Advanced Functional Materials, 2022, 32(36): 2206097.
- [45] Haque A, Liu Y, Karmakar S, et al. Electrochemical performance of carbon-nanotube-supported tubular diamond[J]. ACS Applied Engineering Materials, 2023, 1(8): 2153-2162.
- [46] Deshmukh S, Kunuku S, Jakobczyk P, et al. Diamond based supercapacitors with ultrahigh cyclic stability through dual phase MnO₂ graphitic transformation induced by high dose Mn ion implantation[J]. Advanced Functional Materials, 2023, 34(8): 2308617.
- [47] Geng Z, Cui Z, Liu Y, et al. Electrodeposition ZnO/BDD film as a supercapacitor electrode[J]. Diamond and Related Materials, 2023, 140: 110527.
- [48] Cui Z, Wang T, Geng Z, et al. CoNiO₂/Co₃O₄ nanosheets on boron doped diamond for supercapacitor electrodes[J]. Nanomaterials, 2024, 14(5): 474.
- [49] Liao S, Peng C, Zou J, et al. Boron-doped diamond decorated with metal-organic framework-derived compounds for high-voltage aqueous asymmetric supercapacitors[J]. Carbon, 2024, 230: 119651.
- [50] Cen M, Shao J, Yu S, et al. Cauliflower-like Ni/NiCoP@boron-doped diamond composite electrodes for high-performance symmetric supercapacitors[J]. Diamond and Related Materials, 2024, 149: 111636.
- [51] Xu J, Yang N, Yu S, et al. Ultra-high energy density supercapacitors using a nickel phosphide/nickel/titanium carbide nanocomposite capacitor electrode[J]. Nanoscale, 2020, 12(25): 13618-13625.
- [52] Bogdanowicz R, Dettlaff A, Skiba F, et al. Enhanced charge storage mechanism and long-term cycling stability in diamondized titania nanocomposite supercapacitors operating in aqueous electrolytes[J]. Journal of Physical Chemistry C, 2020, 124(29): 15698-15712.
- [53] Zhang J, Yu X, Zhao Z Y, et al. Influence of pore size of Ti substrate on structural and capacitive properties of Ti/boron doped diamond electrode[J]. Journal of Alloys and Compounds, 2019, 777: 84-93.
- [54] Zhang J, Yu X, Zhang Z Q, et al. Preparation of boron-doped diamond foam film for supercapacitor applications[J]. Applied Surface Science, 2020, 506: 144645.
- [55] Zhang J, Zhao Z, Zhang Z, et al. Construction of flexible fiber-shaped boron-doped diamond film and its supercapacitor application[J]. Journal of Colloid and Interface Science, 2023, 629: 813-821.
- [56] Chen X, Dong X, Zhang C, et al. Interlayer affected diamond electrochemistry[J]. Small Methods, 2024, 9(2): 2301774.

- [57] da Silva L M, de Lima Almeida D A, Oishi S S, et al. Constituent material influence on the electrochemical performance and supercapacitance of PAni/diamond/CF composite[J]. Materials Science and Engineering B, 2018, 228: 249-260.
- [58] Xu J, Yang N, Heuser S, et al. Achieving ultrahigh energy densities of supercapacitors with porous titanium carbide/boron-doped diamond composite electrodes[J]. Advanced Energy Materials, 2019, 9(17): 1803623.
- [59] Long J, Guan L, Wang J, et al. Battery-like flexible supercapacitors from vertical 3D diamond/graphite composite films on carbon cloth[J]. Carbon, 2022, 197: 400-407.
- [60] Suman S, Ficek M, Sankaran K J, et al. Nitrogen-incorporated boron-doped diamond films for enhanced electrochemical supercapacitor performance[J]. Energy, 2024, 294: 130914.
- [61] Jian Z, Yang N, Vogel M, et al. Flexible diamond fibers for high-energy-density zinc-ion supercapacitors[J]. Advanced Energy Materials, 2020, 10(44): 2002202.
- [62] Cui D, Li H, Li M, et al. Boron-doped graphene directly grown on boron-doped diamond for high-voltage aqueous supercapacitors[J]. ACS Applied Energy Materials, 2019, 2(2): 1526-1536.
- [63] Yang N, Jiang X. Rational design of diamond electrodes[J]. Accounts of Chemical Research, 2022, 56(2): 117-127.
- [64] Peng Z, Fiorani A, Tomisaki M, et al. Morphology modulation on boron-doped diamond electrodes and its effect on boosting the conversion of CO₂-to-CO[J]. Diamond and Related Materials, 2023, 138: 110230.
- [65] Otake A, Diaz-Herrezuelo I, Uchiyama K, et al. Fabrication of three-dimensional boron-doped diamond electrodes on SiC scaffolds[J]. Diamond and Related Materials, 2024, 146: 111223.
- [66] Miyake Y, Kondo T, Otake A, et al. Electrochemical CO₂ reduction properties of boron-doped diamond powder[J]. Diamond and Related Materials, 2024, 142: 110821.
- [67] Liu H, Cheng X, You J, et al. Electrochemical reduction of CO₂ using boron-doped diamond electrodes: the influence of deposition times[J]. Functional Diamond, 2024, 4(1): 2301445.
- [68] Du J, Fiorani A, Einaga Y. Electrochemical CO₂ reduction to CO facilitated by reduced boron-doped diamond[J]. Diamond and Related Materials, 2023, 135: 109902.
- [69] Du J, Fiorani A, Inagaki T, et al. A new pathway for CO₂ reduction relying on the self-activation mechanism of boron-doped diamond cathode[J]. JACS Au, 2022, 2(6): 1375-1382.
- [70] Otake A, Du J, Einaga Y. Activation of boron-doped diamond electrodes for

- electrochemical CO2 reduction in a halogen-free electrolyte[J]. ACS Sustainable Chemistry & Engineering, 2022, 10(44): 14445-14450.
- [71] Otake A, Asai K, Einaga Y. Anode reaction control for a single-compartment electrochemical CO₂ reduction reactor with a surface-activated diamond cathode[J]. Chemistry A European Journal, 2024, 30(9): 202302798.
- [72] Luo D, Ma D, Liu S, et al. Electrochemical reduction of CO₂ on fluorine-modified boron-doped diamond electrode[J]. Diamond and Related Materials, 2022, 121: 108753.
- [73] Naragino H, Saitoh Y, Honda K. Electrochemical reduction of carbon dioxide in an aqueous solution using phosphorus-doped polycrystalline diamond electrodes[J]. Electrochemistry Communications, 2022, 134: 107164.
- [74] Injongkol Y, Zhang R Q, Montoya A, et al. Theoretical insights into CO₂ electroreduction on single and dual heteroatom-doped diamonds[J]. Fuel, 2024, 360: 130488.
- [75] Miyake Y, Kondo T, Otake A, et al. Boron- and nitrogen-codoped diamond electrodes for the improved reactivity of electrochemical CO₂ reduction reaction[J]. ACS Sustainable Chemistry & Engineering, 2023, 11(23): 8495-8502.
- [76] Wang H, Tzeng Y K, Ji Y, et al. Synergistic enhancement of electrocatalytic CO₂ reduction to C₂ oxygenates at nitrogen-doped nanodiamonds/Cu interface[J]. Nature Nanotechnology, 2020, 15(2): 131-137.
- [77] Saprudin M H, Jiwanti P K, Saprudin D, et al. Electrochemical reduction of carbon dioxide to acetic acid on a Cu-Au modified boron-doped diamond electrode with a flow-cell system[J]. RSC Advances, 2023, 13(32): 22061-22069.
- [78] Jiwanti P K, Alfaza A M, Kadja G T M, et al. Enhancement of the catalytic effect on the electrochemical conversion of CO₂ to formic acid using MXene (Ti₃C₂T_x)-modified boron-doped diamond electrode[J]. Energies, 2023, 16(12): 4537.
- [79] Jiwanti P K, Alfaza A M, Kadja G T M, et al. Electrochemical study of CO₂ reduction on Ti₃C₂T_x modified boron-doped diamond electrode[J]. Inorganic Chemistry Communications, 2022, 137: 109228.
- [80] Jiwanti P K, Jazuli M A, Sukardi D K A, et al. The effect of SnO-SnO₂ nanoparticle on the carbon dioxide electrochemical reduction activity on MXene/boron-doped diamond (BDD) electrode[J]. Journal of Solid State Electrochemistry, 2024, 29(2): 401-411.
- [81] Bu S, Liu B, Zhu A, et al. Oxygen functionalized diamond nanocone arrays coupling cobalt phthalocyanine for enhanced electrochemical CO₂ reduction[J]. Materials Today Energy, 2024, 44: 101634.
- [82] Conquest O J, Jiang Y, Stampfl C. CoTCNQ as a catalyst for CO₂ electroreduction: A

- first principles r²SCAN meta-GGA investigation[J]. Journal of Computational Chemistry, 2025, 46(1): 27528.
- [83] Mikami T, Yamamoto T, Tomisaki M, et al. Amine-functionalized diamond electrode for boosting CO₂ reduction to CO[J]. ACS Sustainable Chemistry & Engineering, 2022, 10(45): 14685-14692.
- [84] Nihongi S, Otake A, Du J, et al. Convection control in a flow cell on electrochemical CO₂ reduction using a boron-doped diamond electrode[J]. Carbon, 2022, 200: 456-461.
- [85] Irkham, Nagashima S, Tomisaki M, et al. Enhancing the electrochemical reduction of CO₂ by controlling the flow conditions: An intermittent flow reduction system with a boron-doped diamond electrode[J]. ACS Sustainable Chemistry & Engineering, 2021, 9(15): 5298-5303.
- [86] Tomisaki M, Natsui K, Fujioka S, et al. Unique properties of fine bubbles in the electrochemical reduction of carbon dioxide using boron-doped diamond electrodes[J]. Electrochimica Acta, 2021, 389: 138769.
- [87] Araki S, Einaga Y. Semipermanent continuous formic acid production from CO₂ by controlling ion transport using boron-doped diamond electrodes[J]. ACS Sustainable Chemistry & Engineering, 2025, 13(3): 1227-1232.
- [88] Liu B, Zheng Y, Peng H Q, et al. Nanostructured and boron-doped diamond as an electrocatalyst for nitrogen fixation[J]. ACS Energy Letters, 2020, 5(8): 2590-2596.
- [89] Guo Z, Qiu S, Li H, et al. Evaluation of electrocatalytic dinitrogen reduction performance on diamond carbon via density functional theory[J]. Diamond and Related Materials, 2021, 111: 108210.
- [90] Kuramochi S, Fiorani A, Einaga Y. Molybdenum oxide electrodeposition on boron-doped diamond: Investigation of valence state and application in electrochemical nitrogen reduction to ammonia[J]. Diamond and Related Materials, 2023, 139: 110277.
- [91] Zhao Z, Guo K, Zhao Y, et al. Direct N₂ to NH₃ conversion on diamond-supported Ni₄ cluster catalysts: A first-principle study[J]. Surfaces and Interfaces, 2025: 107043.
- [92] Clarke O J R, Rowley A, Fox R V, et al. Diamonds in the rough: Direct surface enhanced infrared spectroscopic evidence of nitrogen reduction on boron-doped diamond supported metal catalysts[J]. Analytical Chemistry, 2023, 95(28): 10476-10480.
- [93] Bandy J A, Zhu D, Hamers R J. Photocatalytic reduction of nitrogen to ammonia on diamond thin films grown on metallic substrates[J]. Diamond and Related Materials, 2016, 64: 34-41.
- [94] Orlanducci S, Ammirati G, Bellucci A, et al. Gold-diamond nanocomposites efficiently

- generate hydrated electrons upon absorption of visible light[J]. ACS Applied Optical Materials, 2024, 2(6): 1180-1187.
- [95] Yoshikawa T, Asakawa H, Matsumoto T, et al. CO₂ reduction by visible-light-induced photoemission from heavily N-doped diamond nano-layer[J]. Carbon, 2024, 218: 118689.
- [96] Su R, Liu Z, Abbasi H N, et al. Visible-light activation of photocatalytic for reduction of nitrogen to ammonia by introducing impurity defect levels into nanocrystalline diamond[J]. Materials, 2020, 13(20): 4559.
- [97] Li S, Bandy J A, Hamers R J. Enhanced photocatalytic activity of diamond thin films using embedded Ag nanoparticles[J]. ACS Applied Materials & Interfaces, 2018, 10(6): 5395-5403.
- [98] Barkl J, Zaniewski A M, Koeck F, et al. Diamond photochemistry with visible light[J]. Diamond and Related Materials, 2019, 96: 195-197.
- [99] Zhu D, Zhang L, Ruther R E, et al. Photo-illuminated diamond as a solid-state source of solvated electrons in water for nitrogen reduction[J]. Nature Materials, 2013, 12(9): 836-841.
- [100] Zhang L, Zhu D, Nathanson G M, et al. Selective photoelectrochemical reduction of aqueous CO₂ to CO by solvated electrons[J]. Angewandte Chemie International Edition, 2014, 53(37): 9746-9750.
- [101] Fayaz H, Ahmad M S, Pandey A K, et al. A Novel nanodiamond/Zinc nanocomposite as potential counter electrode for flexible dye sensitized solar cell[J]. Solar Energy, 2020, 197: 1-5.
- [102] Chen D, Tian B, Fan G, et al. Simple and convenient interface modification by nanosized diamond for carbon based all-inorganic CsPbIBr₂ solar cells[J]. ACS Applied Energy Materials, 2021, 4(6): 5661-5667.
- [103] Zhu Z, Daboczi M, Chen M, et al. Ultrastable halide perovskite CsPbBr₃ photoanodes achieved with electrocatalytic glassy-carbon and boron-doped diamond sheets[J]. Nature Communications, 2024, 15(1): 2791.
- [104] Dong X, Wei Z, Wang T, et al. Insulator-to-metal transition in the black diamond from molecular-dynamics-Landauer method[J]. Optics Express, 2024, 32(3): 3826-3834.
- [105] Girolami M, Bellucci A, Mastellone M, et al. Optical characterization of double-nanotextured black diamond films[J]. Carbon, 2018, 138: 384-389.
- [106] Miliaieva D, Matunova P, Cermak J, et al. Nanodiamond surface chemistry controls assembly of polypyrrole and generation of photovoltage[J]. Scientific Reports, 2021, 11(1): 590.
- [107] Sokeng Djoumessi A, Sichwardt A, Miliaieva D, et al. Nanodiamonds as charge

extraction Layer in organic solar cells: The impact of the nanodiamond surface chemistry[J]. Solar RRL, 2023, 7(12): 2201061.

[108] Ukraintsev E, Kromka A, Janssen W, et al. Electron emission from H-terminated diamond enhanced by polypyrrole grafting[J]. Carbon, 2021, 176: 642-649.

[109] Raymakers J, Krysova H, Artemenko A, et al. Functionalization of boron-doped diamond with a push-pull chromophore via Sonogashira and CuAAC chemistry[J]. RSC Advances, 2018, 8(58): 33276-33290.

[110] López-Carballeira D, Raymakers J, Artemenko A, et al. Effect of oligothiophene spacer length on photogenerated charge transfer from perylene diimide to boron-doped diamond electrodes[J]. Solar Energy Materials and Solar Cells, 2022, 248: 111984.

金刚石相关材料在能量存储与转换中的应用

於思瑜^{1,*},王熙燕¹,杨年俊²

- 1. 化学化工学院,西南大学,重庆,400715,中国;
- 2. Department of Chemistry & IMO IMOMEC, Hasselt University, Diepenbeek 3590, Belgium

摘要:金刚石集多种独特性质于一身,包括优异的稳定性、强光学色散性、卓越的机械强度和极高的热导率。其结构、表面端基和电导性能均具可调控性,进一步增强了其功能多样性。这些特性使金刚石及其相关材料(如复合材料)在能源领域展现出广阔的应用前景。本文综述了金刚石相关材料在能量存储与转换方面的最新研究进展与关键成果,涵盖电化学能量存储(如电池和超级电容器)、电催化能量转换(如CO₂和氦气还原反应)、以及太阳能转换(如光/光电化学CO₂和氦气还原反应,以及太阳能电池)。此外,文章还探讨了金刚石材料在合成及其能源应用中所面临的挑战,并对未来的研究前景进行了展望。

关键词: 金刚石相关材料 电化学储能 电催化能量转换 太阳能转换 未来能源应用方向

基金项目 西南大学中央高校基本科研业务费项目(SWUKT22030),重庆市教育委员会科学技术研究项目(No. KJQN202300205 Deutsche

Forschungsgemeinschaft DFG, German Research Foundation, No. 457444676)

通讯作者/第一作者:於思瑜,副教授.E-mail:yusiyu@swu.edu.cn